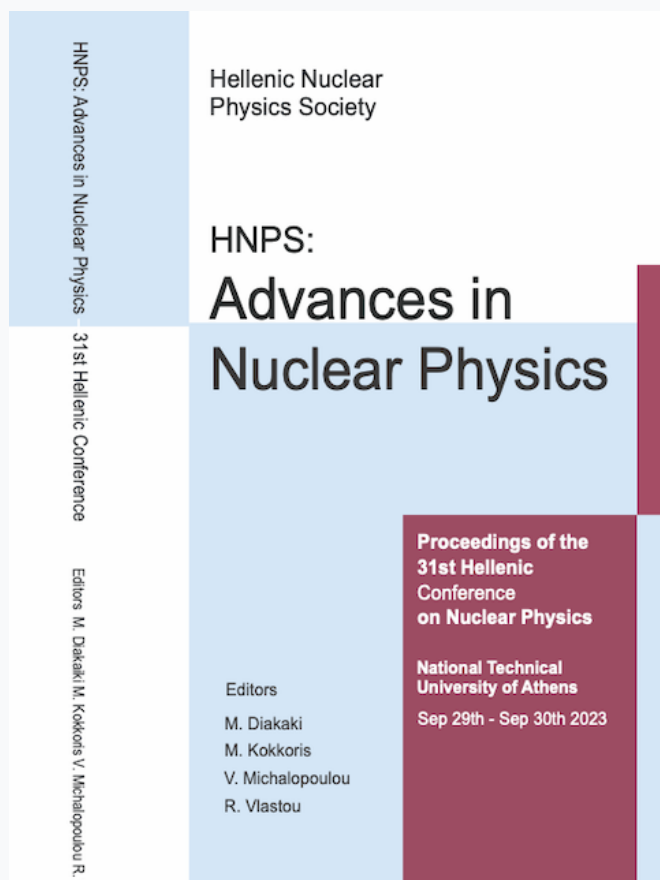


HNPS Advances in Nuclear Physics

Vol 30 (2024)

HNPS2023



Absorbed Dose Distribution in Boron Neutron Capture Therapy for the Treatment of Brain Cancer

Ioanna Koukouletsou, John Kalef Ezra, Evaggelos Pantelis, Antigoni Kalamara, Ion Stamatelatos

doi: [10.12681/hnpsanp.6274](https://doi.org/10.12681/hnpsanp.6274)

Copyright © 2024, Ioanna Koukouletsou, John Kalef Ezra, Evaggelos Pantelis, Antigoni Kalamara, Ion Stamatelatos



This work is licensed under a [Creative Commons Attribution-NonCommercial-NoDerivatives 4.0](https://creativecommons.org/licenses/by-nc-nd/4.0/).

To cite this article:

Koukouletsou, I., Kalef Ezra, J., Pantelis, E., Kalamara, A., & Stamatelatos, I. (2024). Absorbed Dose Distribution in Boron Neutron Capture Therapy for the Treatment of Brain Cancer. *HNPS Advances in Nuclear Physics*, 30, 215–218. <https://doi.org/10.12681/hnpsanp.6274>

Absorbed Dose Distribution in Boron Neutron Capture Therapy for the Treatment of Brain Cancer

I. Koukouletsou^{1,2}, J.A. Kalef-Ezra³, E. Pantelis², A. Kalamara¹ and I.E. Stamatelatos^{1,*}

¹ INRASTES, NCSR "Demokritos", 15310 Aghia Paraskevi, Greece

² Medical Physics Laboratory, Medical School, National and Kapodistrian University of Athens, 11527 Greece

³ Medical Physics Laboratory, School of Health Sciences, University of Ioannina, Ioannina, 45110, Greece

Abstract Boron Neutron Capture Therapy (BNCT) is a promising re-emerging therapeutic approach for brain tumors, such as glioblastoma multiforme, where conventional treatments have limited efficacy. BNCT is based on neutron irradiation of tumors to selectively kill malignant cells that have accumulated boron compounds with high LET particles produced from the thermal neutron absorption reaction in ^{10}B . Two sets of simulations were performed using the MCNP6.1 code. The first involves the study of the dose components as a function of depth in a cylindrical head phantom consisting of water. The second one deals with the estimation of macroscopic dosimetric quantities to the critical structures in the voxelized Zubal anthropomorphic head/neck phantom. Simulations were performed for different neutron energy spectra, beam radii, as well as boron concentrations in the tumor and the surrounding healthy tissues. The findings contribute to the optimized irradiation of the target in BNCT, while sparing of the patient's surrounding healthy tissues.

Keywords cancer therapy, neutron, Monte Carlo simulations, radiation dosimetry

INTRODUCTION

Boron Neutron Capture Therapy (BNCT) is a promising re-emerging therapeutic approach for brain tumors, such as glioblastoma multiforme, where standard treatments have limited efficacy [1]. BNCT is based on neutron irradiation of tumors to selectively kill (either directly or indirectly) malignant cells that have accumulated boron compounds with high LET particles produced by thermal neutron absorption reaction in ^{10}B . Nuclear reactors and accelerators are used to obtain neutron beams with favorable characteristics [2]. Aim of the present study is the estimation of: a) depth-dependent absorbed dose distributions in a cylindrical head phantom composed of light water due to irradiation with neutron beams of various energy distributions and geometries, and b) absorbed dose to various anatomical structures in a voxelized anthropomorphic head/neck phantom.

SIMULATIONS

Simulations were performed using the code MCNP6.1 [3]. The studied neutron energies ranged from thermal up to 14.7 MeV. These included a research reactor thermal neutron beam spectrum taken from [4] and accelerator produced beams utilizing the $^7\text{Li}(p,n)^7\text{Be}$ reaction on a LiF target (0.44 MeV), the $^2\text{H}(^2\text{H},n)^3\text{He}$ reaction (2.87 MeV) and the $^3\text{H}(^2\text{H},n)^4\text{He}$ reaction (14.73 MeV). The accelerator spectra were calculated using the NeuSDesc code [5]. Simulations were performed for beam radii, r_s , ranging from 1 cm to 7.5 cm. The ENDF/B-VII.1 cross section data library was used, in conjunction with the LWTR.01T thermal neutron treatment for light water. The total energy deposition in MeV/g, the energy deposition of all particles except photons in MeV/g and the photon energy deposition in MeV, per incident neutron, were calculated using tallies F6, +F6 and *F8, respectively. In the Zubal phantom neutron KERMA (cGy), boron absorbed dose (cGy/ppm ^{10}B) and photon absorbed dose (cGy), to the brain and head structures given in reference [6] were calculated using the ICRU 46 [7] dosimetric

* Corresponding author: ion@ipta.demokritos.gr

factors.

PHANTOM CHARACTERISTICS

The homogeneous head phantom consisted of a light water cylinder 20 cm in diameter and 20 cm in height. Cylindrical detectors of 2 cm in diameter and 0.5 cm in height were positioned along the main axis of the cylinder. The Zubal head and neck phantom is a high-resolution voxelized anthropomorphic phantom consisting of 32 anatomical structures of the head and neck [8]. The simulated tissues included adipose tissue, eye lens, muscle, cranium skeleton, spongiosa skeleton, cartilage skeleton, skin, brain-gray matter, brain-white matter, cerebrospinal fluid, eyes and spinal cord. A cross section of the the homogeneous and Zubal phantom used in this study is shown in Figs. 1a and 1b, respectively.

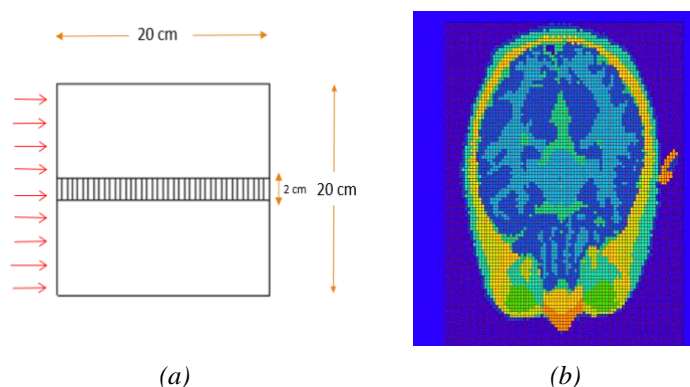


Figure 1. Head phantoms used (a) homogeneous water phantom and (b) Zubal anthropomorphic phantom

RESULTS AND DISCUSSION

Fig. 2(a-d) shows the predicted absorbed dose from all particles as a function of depth along the main axis of the cylindrical phantom for the neutron sources and beam radii examined. The smaller the beam radii is, the lower the deposited energy along the main axis of the cylindrical phantom. Increasing beam radius results in increased neutron elastic scattering mainly in hydrogen and therefore in increased energy deposition along the beam axis. The lower the average kinetic energy of the neutrons in the beam, the stronger the dose gradient and the faster the dose decrement.

Fig. 3 (a-d) shows the absorbed dose per ppm of ^{10}B to the structures given in the Zubal phantom in a case of a cephalocaudal thermal neutron irradiation ($r_s=12.5$ cm). Increase in the beam radius, decreases the absorbed dose per incident neutron for those organs in the supraventricular region (upper part of the brain), with the exception of optic nerves. However, this reflects in the normalization per incident neutron. As field size increases, so does the absorbed dose to the extracranial organs, the cerebellum, the optic nerve and the medulla oblongata (Fig. 3d), since they are now within the view of the beam. The absorbed dose distribution in the Zubal phantom depends on the anatomical position, the elemental composition, the density and spatial ^{10}B concentration, as well as the neutron energy spectrum and beam size. Increase in the neutron energy increases the dose absorbed in organs at greater depths.

Application of the data provided in Fig. 3 allows the calculation of an index of the absorbed dose in critical brain and head structures. For example, in Table 2 neutron KERMA, boron absorbed dose, photon absorbed dose and the gamma equivalent dose assuming a 2.5 value for the high LET radiations are given for structures and organs in case of a craniocaudal thermal neutron field (1×10^{12} cm $^{-2}$ in flux and 12.5 cm in radius), assuming a uniform 30 ppm ^{10}B brain concentration (tumor) and 6 ppm in the remaining organs (healthy tissues) [9].

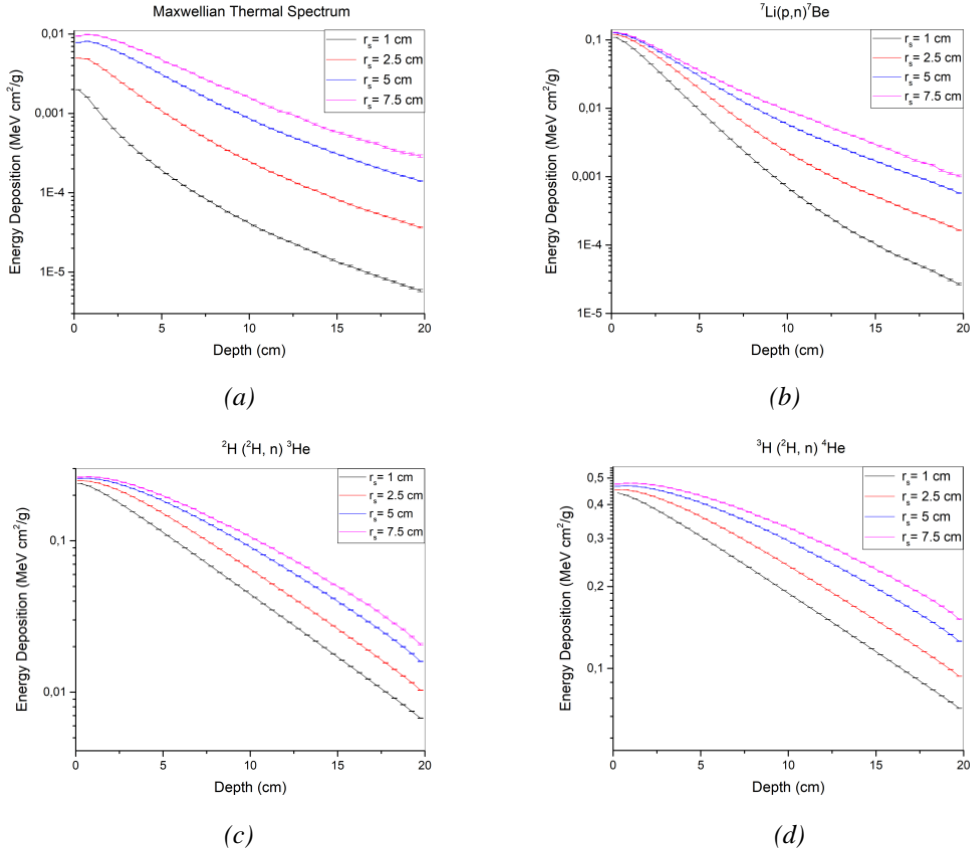


Figure 2. Energy dissipation from all particles with depth in an homogeneous cylindrical head phantom for the neutron sources examined

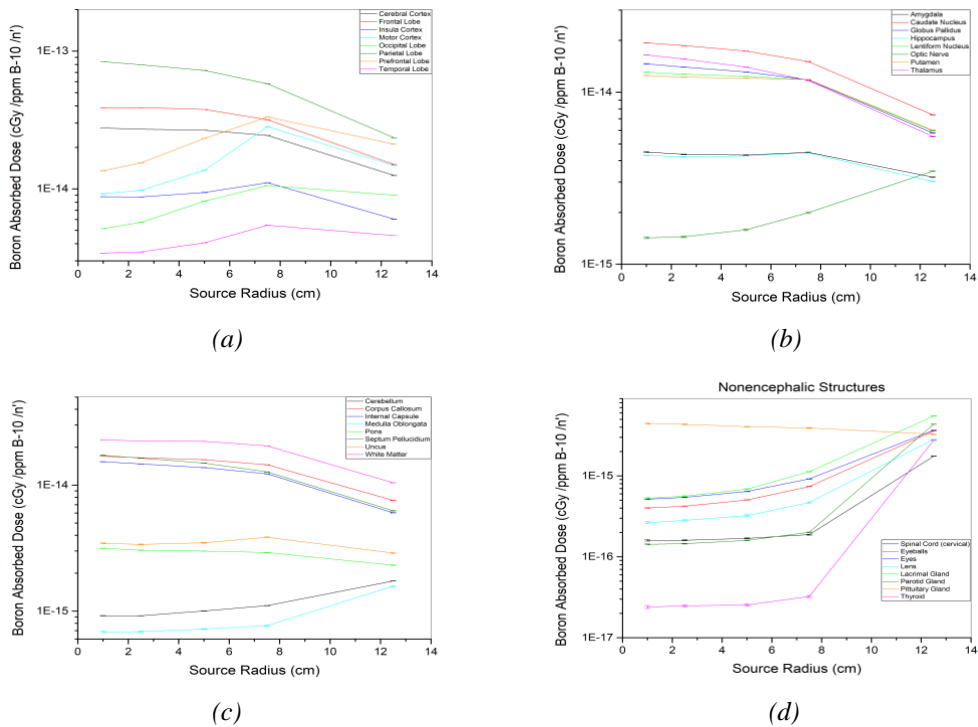


Figure 3. Boron absorbed dose for different brain structures (a, b, c) and non-encephalic structures (d) with different field sizes in case of a cephalocaudal thermal neutron irradiation ($r_s=12.5$ cm) of the anthropomorphic head phantom (Normalization per source neutron)

Table 2. Neutron KERMA, boron absorbed dose and photon dose to some anatomical head/neck structures of the Zubal phantom in case of a cephalocaudal thermal neutron beam of 1×10^{12} n·cm⁻², 12.5 cm in radius

| Structure | ¹⁰ B (ppm) | KERMA (cGy) | Boron Absorbed Dose (cGy) | Photon Absorbed Dose (cGy) | Total Absorbed Dose (cGy) | γ-equivalent Dose (Gy _{eq}) |
|-----------------|-----------------------|--------------|---------------------------|----------------------------|---------------------------|---------------------------------------|
| Parietal lobe | 30 | 41.34 ± 0.03 | 1120.6 ± 0.80 | 385.40 ± 0.50 | 1547.3 ± 1.3 | 32.90 |
| Cerebral Cortex | 30 | 26.04 ± 0.05 | 706.5 ± 1.60 | 282.20 ± 1.10 | 1014.7 ± 2.8 | 21.14 |
| Thalamus | 30 | 9.76 ± 0.03 | 264.0 ± 0.80 | 232.00 ± 0.90 | 505.8 ± 1.7 | 9.16 |
| Cerebellum | 30 | 3.06 ± 0.09 | 82.84 ± 0.22 | 117.88 ± 0.27 | 203.7 ± 0.6 | 5.33 |
| Eyes | 6 | 4.99 ± 0.02 | 35.90 ± 0.14 | 124.40 ± 0.60 | 165.3 ± 0.8 | 2.27 |
| Thyroid | 6 | 5.25 ± 0.02 | 26.27 ± 0.10 | 110.00 ± 0.50 | 141.5 ± 0.8 | 1.89 |
| Spinal Cord | 6 | 3.08 ± 0.02 | 16.70 ± 0.08 | 103.60 ± 0.70 | 123.4 ± 0.8 | 1.59 |

CONCLUSIONS

Addressing the numerous parameters found in BNCT is a challenge. Monte Carlo calculations are an important tool in dosimetry, offering the possibility of interpreting and evaluating data with high-dose gradients, which would not be easy to study experimentally. The example given shows clearly one of the reasons for the failure of early clinical trials to treat deep-sitting brain tumors with BNCT using thermal neutron beam [10]. Thus, it may contribute to the optimization of the irradiation parameters and the need for use of neutron beams of optimized characteristics.

References

- [1] M.A. Dymova et al, Cancer Commun. 40, 406 (2020); doi: 10.1002/cac2.12089
- [2] R.L. Moss, Appl. Radiat. Isot. 88, 2 (2014); doi: 10.1016/j.apradiso.2013.11.109
- [3] Initial MCNP6 Release Overview MCNP6 Version 1.0, Los Alamos National Laboratory report LA-UR-13-22934 (2013).
- [4] IAEA, Compendium of Neutron Spectra and Detector Responses for Radiation Protection Purposes, TRS-403, Vienna, 2001, ISBN 92-0-102201-8
- [5] E. Birgersson and G. Loevestam, NeuSDesc-Neutron Source Description Software Manual. EUR 23794 EN. Luxembourg: OPOCE, 2009, JRC51437
- [6] J.F. Evans et al, Med. Phys. 28, 780 (2001); doi: 10.1118/1.1354997
- [7] ICRU, Photon, electron, proton and neutron interaction data for body tissues, Report 46, Washington: International Commission on Radiation Units and Measurements (1992)
- [8] I.G. Zubal, Med. Phys. 21, 299 (1994); doi: 10.1118/1.597290
- [9] R.G. Fairchild et al, Med. Phys. 17, 1045 (1990); doi: 10.1118/1.596455
- [10] D.N. Slatkin et al, Neurol. Neurobiol. 3.2 (2017); doi: 10.16966/2379-7150.142